Fundamental aspects of HCOOH oxidation at platinum single crystal surfaces with basal orientations and modified by irreversibly adsorbed adatoms.

A. Boronat-González, E. Herrero*, J.M. Feliu*

Institute of Electrochemistry. University of Alicante. Apdo. 99. E-03080 Alicante. Spain.

*herrero@ua.es, **juan.feliu@ua.es

Abstract.

Oxidation of formic acid at Pt(hkl) electrodes with basal orientations and modified by irreversibly adsorbed adatoms is revisited. It was shown that the adatoms of the nitrogen group could enhance the electrocatalytic activity through long range electronic effects in the case of Pt(111) substrates or through shorter third body effects when adsorbed at Pt(100) electrodes. In both cases it appears that free platinum sites were required. Special attention is given here to the reactivity at Pt(110) substrates. It is found that maximum electrocatalysis is observed at fully blocked surfaces. This result points out again structure sensitivity effects for this characteristic reaction. Unlike the more compact planes, in which the enhancement of the oxidation rate was explained through essentially rigid models for the adlayer, it is suggested that the resulting enhancement observed at Pt(110) substrates could be explained if some adatom mobility is considered.

Key words: Formic acid oxidation; surface reactivity; Pt single crystals; irreversible adatom adsorption.

1. Introduction.

Formic acid oxidation reaction has been studied widely due to the possible use of formic acid as a fuel in fuel cells. As compared to other possible organic fuels, it has one of the lowest energy densities, since only two electrons are exchanged in the oxidation process. However, the main advantage in the use of formic acid is that the known electrocatalysts, always noble metals and their alloys or compounds, provide higher currents at low overpotentials than the other organic fuels, resulting in an overall higher power for a given mass of noble metal in the fuel cell. The key issue in the facile electrocatalysis of the formic acid oxidation reaction is that only two electrons are exchanged, resulting in a simpler mechanism.

The reason of this can be deduced when this reaction is compared with the ethanol oxidation reaction. To oxidize ethanol to two CO_2 molecules, three different type of processes are required: the C-C bond cleavage, the dehydrogenation of the carbon groups and the transfer of the oxygen required. From the mechanistic studies, it has been observed that platinum is very active for the dehydrogenation processes of the carbon groups, giving rise to the formation of adsorbed CO. However, it is not very effective in the cleavage of the C-C bond or the transfer of the oxygen groups, necessary for the oxidation of CO to CO_2. For this latter process, ruthenium or other adatoms are added to the surface of the platinum catalysts to facilitate its oxidation. In the case of formic acid oxidation, the most difficult steps for a platinum electrocatalyst are not involved in the process, since the molecule has only one carbon and it contains all the oxygen atoms required for the oxidation to CO_2. For that reason, platinum performs better for this reaction than for methanol or ethanol oxidation.

In spite of the apparent simplicity of the process, that is the oxidation only requires the elimination of two hydrogen atoms in the form of protons and the transfer of the two

corresponding electrons, the oxidation mechanism has a double pathway. This pathway was introduced by Capon and Parsons in 1973 [1] and later confirmed by DEMS [2]. The scheme of this mechanism is the following:

$$\text{HCOOH} \begin{cases} \text{Active Intermediate (AI)} \xrightarrow{E_1} CO_2 + 2H^+ + 2e^- \\ \qquad\qquad\qquad\qquad\qquad\qquad\qquad\qquad E_2 > E_1 \\ CO + H_2O \xrightarrow{E_2} CO_2 + 2H^+ + 2e^- \end{cases}$$

The first route, that going through the active intermediate, would be the "natural" route, because it is simplest one. Formic acid adsorbs on the surface, probably transferring one electron, to form of an active intermediate, and then this intermediate is oxidized to CO_2. Regarding the nature of the active intermediate, the question is not yet fully resolved [3-5]. It has been proposed that the active intermediate is adsorbed formate, but other experiments seem to contradict that observation [6-10].

In the second pathway, the first step in this route is a dehydration step with the loss of an oxygen atom to form adsorbed CO. Precisely, the transfer of this oxygen atom back to the carbon is the most difficult step in the CO oxidation process. In addition, CO adsorbs strongly on the surface, and for that reason, this route is also known as the poisoning route and, therefore, the other one as the active intermediate route. This way, adsorbed CO blocks the active sites of the surface and prevents the advance of the oxidation reaction.

On platinum, both routes are structure sensitive and there is a clear dependence of the reactivity on the surface structure, as the experiments with single crystal electrodes demonstrate [11]. However, the activity of both routes seem to follow the same trend. Pt(111) is the less active single crystal electrode surface both for the active intermediate route and the CO route. On the other hand, Pt(100) shows a much higher activity for both processes. Additionally, both routes appear to have different site requirements, since the presence of a blocking species on the active sites seem to affect more significantly the route through CO

than that through the active intermediate [12,13]. For that reason, it is proposed that this route requires at least two contiguous platinum sites to proceed.

From that description, the ideal electrocatalysts would be the one that accelerates the active route and prevents the formation of CO. Several strategies has been adopted to reach those goals, but in general, they consists in the modification of platinum with a second element. This modification can consist in deposition of submonolayer amounts of an element [14-16], the deposition of metallic monolayer [17] or the formation of alloys or intermetallic compounds [18-20]. These modifications of the platinum can act in two different ways: it can prevent the formation of CO through a third body effect, resulting in an increase in the overall reactivity due to the larger availability of active sites for the active intermediate route, or, it can increase the catalytic activity of the active intermediate route through an electronic effect [21].

In this manuscript, results from the group regarding formic acid oxidation will be reviewed, to gain insight into the process. The kinetics of both routes on platinum single crystal electrodes will be examined to determine the effect of the surface structure on both routes. Using these results, it will be possible to determine the exact role of the adatoms in the formic acid oxidation reaction.

2. Experimental.

Platinum single crystal electrode surfaces were prepared from small single crystal beads, *ca.* 2 mm in diameter following the method developed by Clavilier [22]. Before any experiment, working electrodes were annealed for around 30 s in a gas oxygen-flame, cooled down in a reductive atmosphere (H_2 + Ar) and quenched in ultrapure water in equilibrium with this atmosphere [23]. Then, the electrodes were transferred to a cell under the protection of a droplet of deoxygenated water for further characterization.

All experiments were carried out at room temperature in a typical three-electrode electrochemical cell. A platinum wire was used as a counter-electrode and a reversible hydrogen (N50, Air Liquide) electrode (RHE) was used as a reference. Solutions were prepared from sulfuric acid (Merck 95-97% GR for analysis), formic acid (Merck p.a.) and ultra-pure water (Elga-Purelab Ultra 18.2 MΩ cm). Argon (N50, Air Liquide) was used for deoxygenating all the solutions.

3. Effect of the surface structure on the two routes for formic acid oxidation.

As can be seen in figure 1, formic acid oxidation is a structure sensitive reaction. For the Pt(100) electrode, the current is very low in the positive going scan, since CO has been formed at low potentials and has blocked the surface. Above 0.7 V, CO is readily oxidized and the surface recovers its full activity. In the negative scan, currents are much higher, since the surface is free from adsorbed CO at potentials higher than 0.5 V. In the case of the Pt(111) electrode, currents are much lower, which indicates a lower activity for the direct oxidation of formic acid, but the hysteresis is also much smaller. Since the the maximum coverage for CO obtained from formic acid is very similar for both electrodes [24,25], the lower hysteresis should be then related to a slower kinetics of CO formation.

Although voltammetry can be used to have a qualitative assessment of the activity for formic acid oxidation and the effects of the surface structure in the two routes, obtaining quantitative data requires a very complex analysis and simulation. The major problem for the quantitative analysis is that the electrode potential is time dependent, so that the measured currents not only depends on the potential but also on the previous history of the electrode potential. As aforementioned, the amount of adsorbed CO on platinum at a given potential in voltammetry depends on the scan direction, giving rise to hysteresis in the voltammetry. A much better approach for that is recording chronoamperometric transients at different

potentials, measured always in the same conditions. This is the principle of pulsed voltammetry, which was initially devised by Clavilier [26]. In initial version of this technique, a short pulse at high potential was superimposed to a normal voltammetric potential sweep. CO was oxidized in this short pulse, and, when the potential was set back to the previous value, the initial oxidation current corresponds to that measured in the absence of CO on the surface. In order to simplify the analysis, a modification was proposed [27,28], in which the potential was kept constant between steps.

The analysis of the transients can be made taking into account the kinetics of the two routes. For the active intermediate route, the current depends only on the fraction of the surface not covered by CO, so that:

$$j = j_{\theta=0}\left(1-\theta_{\mathrm{CO}}\right) \qquad (1)$$

where $j_{\theta=0}$ is the intrinsic activity of the surface, which corresponds to the current density that should be measured when θ_{CO}=0, and θ_{CO} is the CO coverage defined as the fraction of the surface covered by CO.

For the poisoning route, it was experimentally observed that CO is only formed at potentials below 0.6 V, so that CO oxidation is not possible. Thus, only the reaction

$$p\ \mathrm{Pt} + \mathrm{HCOOH} \rightarrow \mathrm{Pt_p\text{-}CO} + \mathrm{H_2O} \qquad (2)$$

will be considered. Here p represents the number of Pt reaction sites required for the reaction to occur. The corresponding kinetic equation for this reaction is

$$\frac{\mathrm{d}\theta_{\mathrm{CO}}}{\mathrm{d}t} = k_{ads}\left(1-\theta_{\mathrm{CO}}\right)^{p} \qquad (3)$$

where k_{ads} is the constant rate for the formation of CO from formic acid. The integration of this equation will give the evolution of the CO coverage with time. The substitution of θ_{CO} in equation (1) gives

$$j = j_{\theta=0}\left(\frac{1}{1+k_{ads}t(p-1)}\right)^{\frac{1}{p-1}} \quad (4)$$

This equation gives rise to transients in which the current diminishes with time. At t=0, the current is equal to $j_{\theta=0}$, so that the extrapolation of the measured currents to t=0 will be used to measure this parameter. The diminution with time is proportional to k_{ads}. The larger k_{ads} is, the faster decay is observed. In all the fittings carried out with the model, the values of p for the transients with a measurable CO formation rate are always close to two. This value indicates that the formation of CO from formic acid requires two platinum sites [27]. Conversely, it has been shown that the direct oxidation of formic acid can take place on isolated Pt sites [13,21], and therefore it can be concluded that the site requirements for CO formation are higher than those needed for the direct oxidation.

Using this analysis, the effect of the surface structure on both routes was examined on platinum single crystal electrodes vicinal to the (100) and (111) pole. A summary of these results is presented in figure 2. First of all, the values of $j_{\theta=0}$ show a clear effect of the surface structure. For the Pt(100) electrode and the surfaces vicinal to this pole, the onset for the oxidation is ca. 0.3 V and reaches a maximum value at 0.40 V, exhibiting large currents [27,29]. For short terraces, the current for the active intermediate route diminishes, a can be seen for the Pt(311), surface which is the turning point in the series. On the other hand, the Pt(111) electrode has a similar onset for formic acid oxidation, but currents are ca. 20 times smaller than those recorded for the Pt(100) electrode. Additionally, the presence of steps on the (111) terraces does not increase the catalytic activity of the surface, since current are smaller than those measured for the Pt(111) electrode and the onset is displaced towards lower potential values. The only exception to this rule is the Pt(311) surface, which shares some characteristics of the surfaces pertaining to the (100) pole.

A similar situation is observed for the values of k_{ads} (figure 3). In some cases, the pulse sequence was modified to measure it in regions where currents for the direct oxidation were negligible [28]. The first remarkable result is that the constant rates for CO formation on the Pt(111) electrode are well below the limit of detection of the technique employed (<0.01 s^{-1}). This means that the Pt(111) electrode was virtually inactive for the formation of CO. The addition of steps to the (111) terraces leads to the formation of CO in two different and narrow potential regions. For the (110) steps, formation of CO occurs around ca. 0.15 V whereas for the (100) steps is around 0.25 V. Both potentials regions corresponds to the potential of total zero charge of the both type of steps on the (111) terrace [30,31]. The results obtained with the Pt(111) electrode and the vicinal surfaces confirm previous hypothesis: steps and defects are responsible for the formation of CO from formic acid on surfaces having (111) terraces [32-34]. For the surfaces vicinal to the (100) pole, CO formation occurs around 0.38 V, which is also very close to the potential of zero charge of these electrodes [27]. It has been suggested that the close relationship between the CO formation and the pztc indicates that the required interaction between the formic acid (or formate ion) and the surface should be weak since this the type of interaction is obtained in the neighborhood of the pztc [27].

As a summary, the order of reactivity of the different for the direct oxidation reaction according to the measured currents for $j_{\theta=0}$ is the following: (100) terraces≈ (111) steps on the (100) terraces>>(111) terraces>(110) steps on (111) terraces>(100) steps on (111) terraces. For the CO formation, taking into account the maximum rate observed, independently of the potential, the order is (100) terraces≈ (111) steps on the (100) terraces >(110) steps on (111) terraces>(100) steps on (111) terraces>>(111) terraces. In this latter case, it should be taken into account that only for (100) terraces and for (111) steps on the (100) terraces, the region where the CO formation takes place coincides with the region in which significant currents for the oxidation are measured. On the other hand, for (110) and

(100) step sites on the (111) terrace domains, no CO formation is detected in the regions where measurable oxidation currents are observed. For that reason, the decay for the transients with measurable oxidation currents is negligible for electrodes close to the (111) pole. This effect would suggest that a practical electrode with no (100) terrace sites under working conditions in a fuel cell would have no poisoning once all the CO formed during start up processes has been oxidized.

4. Formate adsorption.

The role of formate in the oxidation mechanism of formic acid has be the subject of a strong debate [3-5]. In order to shed some light to the problem, fast scan experiments for formic acid oxidation in perchloric acid solutions were carried out. The advantage of the fast scan rates is that the current for formic acid oxidation is almost independent of the scan rate, whereas the currents for pseudo-capacitive processes, such as those related to the adsorption of anions, are directly proportional to the scan rate. At 50 V s^{-1}, the currents measured for the oxidation are negligible when compared to that corresponding to adsorption processes [35]. Thus, it was possible to detect adsorbed formate on the surface. In fact, the measured voltammetrc profile at such high scan rates was very similar to that recorded in acetic acid solutions. Additionally, the coverage was proportional to the measured currents in the region between 0.4 and 0.6 V, which clearly indicates that adsorbed formate has a key role in the oxidation of formic acid.

5. Effect of the adatoms in the route through CO.

The adsorbed atoms on the electrode surface can have three different mechanisms through which they alter the catalytic activity of the underlying surface: i) third body effect, ii) electronic effect and iii) bifunctional effect. In the third body effect, the adatom acts a mere

spectator, and only blocks surface sites, diminishing the activity for the undesired reaction. For the other two effects, the adatom has an active role in the catalytic process, either it modifies the electronic properties of the surface so that the reactivity of the surface changes in the electronic effect or it transfer a required group for the reaction to occur in the bifunctional catalysts. A typical case for the bifunctional catalyst is the CO oxidation on Pt surface activated by the presence of surface ruthenium. In this case, the large ability of Ru for the adsorption of OH helps in the oxidation of CO to CO_2 by transferring the OH group adsorbed on Ru to the CO molecule adsorbed on Pt. For formic acid oxidation, the transfer of an additional group is not necessary, so that the bifunctional mechanism will not be considered.

The initial studies on the effect of the modification of the Pt(111) electrode by Bi, As, Te or Sb appeared to suggest that those adatoms had a large electronic effect inhibiting the CO formation route [24,36,37]. Very low coverages (below 0.04) of those adatoms were able to completely eliminate CO formation from formic acid [24]. On the other hand, Se adatoms showed the typical third body effect [38,21] in which complete inhibition only occurs at coverages close to the maximum value for a single layer. However, the studies with stepped surfaces demonstrated that the origin of such “striking” long-range effect was different, since the route through CO is confined to the defects on the surface on the Pt(111) electrode [32-34,28]. On a Pt(111) terrace, Bi, As or Te adsorb preferentially on the steps or defects, whereas Se or S do not show that preference [39]. The different behavior regarding the adsorption on the (111) terraces of Bi, As or Te as compared with Se or S was related the different surface dipole created upon adsorption on the (111) surface. Bi, As or Te, when adsorbed, are more positive than the Pt atoms which guides their adsorption to the lower part of the step, which have an excess of negative charge. On the other hand, S or Se are more negative than the surface and therefore have no tendency to adsorb on those sites. Since the amount of defects present in a bead-type Pt(111) electrode is very low, very small amounts of

those adatoms (Bi, As, or Te) are required to block those sites and completely inhibit CO formation from formic acid. Thus, the apparent long-range electronic effect is just a mere third body effect in which the number of sites performing the undesired reaction is very low and the adatoms block initially only these sites.

For the surfaces belonging to the Pt(100) pole, the adatoms always behave as a third body [25,12]. For these surfaces, CO formation occurs throughout the surface [27,29] and the adatoms do not adsorb preferentially on any type of site [40,41], giving rise to the typical third body effect for the formation of CO.

6. Effect of the adatoms in the route through the active intermediate.

As before, the adatoms can have two different effects on this route: third body or electronic effects. As has been described in the previous section, the presence of adatoms diminishes the rate the route through CO through a third body effect. It has been demonstrated that the number of neighboring sites required to the dehydration step to occur is higher than those necessary for the direct route [38,21,13]. In fact, in the proposed model for fitting the transients, the formation of CO requires two sites whereas the direct route only need one platinum site [27]. It is possible, then, to distribute the adatoms over the surface in such a way that only isolated Pt sites are found [42]. Under those conditions, direct oxidation still occurs but CO formation is completely inhibited and an apparent increase in the oxidation currents observed by voltammetry is possible [43,14]. This increase is only due to a lower accumulation of CO on the surface [21]. Thus, currents increase as the coverage increases until the adatom reaches a value of ca. 0.7-0.8 of the maximum coverage. From that point, the current sharply diminishes due to the total blockage of the Pt sites, which are required to oxidize the formic acid molecules.

A similar behavior is also be obtained if the adatom play an electronic effect on the reaction. The catalytic site is the Pt atom close to an adatom, and since the free Pt and the adatom are required to oxidize the molecule a maximum activity is obtained for coverages of ca. 0.7-0.8 of the maximum coverage [21]. The only way to distinguish whether the adatom is playing an electronic effect for the direct route is by comparing the measured currents with those obtained for the unmodified surface in the absence of CO on the surface, that is, with $j_{\theta=0}$. If the measured currents in the presence of an adatom are higher than $j_{\theta=0}$ for the unmodified surface, a clear electronic effect is present for the direct route. If not, the adatom is probably playing a third body effect also for this route.

For the Pt(111) electrode and vicinal surfaces modified with Bi, As, Te, Sb or Pb a clear increase in the currents with respect to those measured in the clean surface is observed [15,44,45,36,46,47,37,48]. For instance, the currents for a Bi modified surface can be 40 times higher than those measured for the unmodified surface in the absence of poison at the same potential. In fact, Bi or Pb are the adatoms with a higher catalytic effect for this reaction. It should also be hihglighted that Pb on the Pt surface has a low stability. On the other hand, Se only plays a pure third body effect for the direct route [38].

For the Pt(100) surfaces, the effect of the adatoms is less pronounced. The measured currents are lower than $j_{\theta=0}$ for the clean Pt(100), so that the presence of an electronic effect cannot be confirmed. Only in the case of Sb, currents for high coverages are comparable with $j_{\theta=0}$ [16,21] and so the adatom essentially plays the role of a third body. If the currents are normalized to the number of Pt sites, a moderate increase in the activity is observed, but this increase is much less pronounced than that measured for the Pt(111) electrode.

7. Oxidation of formic acid on Pt(110) modified electrodes.

Unlike the other basal planes, Pt(110) has been less investigated despite of the fact that a significant fraction of surface sites with this orientation is present at polycrystalline platinum. In this respect, it might be surprising to realize that the study of vicinal surfaces to the Pt(110) pole is only recently accomplished [49]. One of the main problems with the use of this surface plane of low atomic density deals with possible reconstruction phenomena, which is well documented in ultrahigh vacuum. The first electrode pretreatments after flame annealing were made by cooling and quenching in air, but later the reductive hydrogen atmosphere was used, as done with Pt(100) electrodes [50]. It appears that the air-cooling step leads to a characteristic double peak voltammetric profile [51], but the surface is not well ordered. In electrochemical environments, the effect of the cooling step was highlighted using synchrotron radiation [46]. It was found that the surface structure was dependent of the cooling rate under reductive conditions: fast cooling would lead to the (1×1) structure and sharp voltammetric peaks in the hydrogen region, whereas slow cooling would result in the (2×1) reconstruction and broader peaks, but appearing in the same potential region [52]. This constant value of the peak potential is makes difficult to electrochemically discriminate one of the two structures in an absolute way. Likely mixtures of both types of domains exist on the surface in all cases. In this respect STM studies have not been able to characterize the Pt(110)/ solution interface [53]. In this later study, it was suggested that the cooling in CO atmosphere leads to better ordered surfaces. The effect of CO adsorption in the definition of the voltammetric profile was earlier observed in CO displacement experiments, either with hydrogen or air cooled samples [54] and recent results also suggest that this type of treatment is convenient to produce well-ordered samples [55]. The use of poisonous CO in the treatment is dangerous and it would be good to replace it by other species. In summary, it seems that reductive atmospheres are required in the treatment and this leads to the observation of sharp voltammetric peaks at 0.13 V in 0.5 M sulfuric acid, jointly with small currents at potentials

higher than 0.2 V (likely belonging to small [56] domains). This voltammetric profile would characterize a state of the art for the Pt(110) electrodes that contains likely about 50% of long range (1x1) bidimensionally ordered domains separated by smaller {110} and {111} ones [49].

This heterogeneity in the surface domains seems to be a characteristic of the Pt(110) surface under electrochemical environments, in which potential cycling is required in order to characterize the surface by structure sensitive reactions. It is known that both potential and adsorbates can modify the surface structure. It can be expected that the final stable surface obtained in the potential range that excludes electrochemical adsorption oxygen, is determined mainly by the anneling step (temperature and quenching atmosphere). In the following, the electrochemical properties of the (1×1) structure, fulfilling the criteria described above, have been used to define the starting point of the substrate and few potential cycles have been used in order to disturb the surface as less as possible.

Another problem dealing with the electrochemical characterization of Pt(110) is the elevated charge measured under the voltammogram, 220 μC cm^2 in 0.5 M sulfuric acid, which exceeds by 50% the nominal monoelectronic transfer for a monolayer of adsorbed hydrogen. Although this excess of charge would agree with the excess of surface atoms present in the (2×1) reconstruction, the CO displacement experiment showed that the charge excess is due to sulfate adsorption following hydrogen desorption. The charge for sulfate adsorption has to be added to the charge corresponding to the likely fully covered hydrogen adlayer, which amounts to 150 μC cm^2 [57]. Incidentally, the charge density values and the resulting potentials of zero total charge values are almost independent of the voltammetric shape, i.e. sharp peaks characteristic of the (1×1) structure, broader peaks assigned to the (2×1) reconstruction or double peaks that are characteristic of the air cooled surfaces and correspond to more disordered surfaces.

The main drawback to the use of Pt(110) in model electrocatalytic studies with adatoms is that the redox process undergone by the irreversibly adsorbed species appears at high potentials, overlapping with the surface oxidation [58]. This would mean that a balance of the charge in the low potential region, assigned to the platinum free sites, versus the adatom redox charge could not be made, because the latter charges would also contain a contribution coming from the adsorption of oxygenated species at the platinum free sites. This fact makes difficult an appropriate charge balance for the adatom redox process and would not supply calibration plots useful to discard experiments in which occasional contaminants could be incorporated to the surface during the electrode handling step necessary to generate the irreversible adsorbed layer. This is still true today, but the expertise gained in this type of electrode manipulation with Pt(111) and Pt(100) substrates, in which detailed charge balances can be made, jointly with the understanding of the appropriate surface pretreatment allow discarding the presence of that foreign contaminant contributions and validates the results obtained here.

Regarding the lack of reliable calibration curves, it should be mentioned that this does not have influence in electrocatalytic-related parameters such as adatom surface coverage determination. From the aforementioned reasons, it is clear that a satisfactory surface stoichiometry for the adatom redox reaction cannot be surely established, but adatom coverage can be measured through the blockage of the platinum sites, following the general expression [59]:

$$\theta_{Ad} = 1 - \theta_{H} = 1 - \frac{Q_{Pt}}{Q^{o}_{Pt}} \qquad (5)$$

where θ_{Ad} represents the adatom coverage as a function of the platinum coverage in the hydrogen region (hydrogen and anion coverage), oversimplified as θ_H. The latter value is measured as the ratio of the charges in the low potential range from the adatom covered surface and the blank electrode after the flame treatment, Q_{Pt} and Q^{o}_{Pt}, respectively. This

would consider, however, that the hydrogen and anion adsorption charge contributions in the partially covered Pt(110) surfaces are proportional to those at the Pt(110) clean surface after flame treatment. With all these cautions, the use of Pt(110) modified by adatoms as model surfaces to understand electrocatalytic reactivity can be considered. Despite of the experimental uncertainties, a different reactivity of these electrodes as the coverage increases will be clearlypointed out: In this case, the most catalytic surfaces are those fully covered by the adatoms, a behavior not generally observed with the other two basal planes investigated earlier.

Regarding the oxidation of formic acid, it should be stated that formic acid oxidation at Pt(110) is almost negligible at potentials below 0.75 V (figure 4). The surface is almost completely blocked by linearly adsorbed CO [60] and only after excursion to 0.95 V it is possible to notice the presence of a small oxidation peak in the positive-going sweep. In the negative-going sweep the surface is quite reactive at lower potentials showing a classical hysteresis loop related to poison elimination. It should be noted that surfaces treated under reductive conditions are quite stable in successive cycles, unlike that observed with air treated samples. This is likely due to the fact that the latter surfaces are more disordered and that CO adsorption and stripping modifies its structure in a progressive way, as mentioned above [49].

The voltammetric profile of Pt(110) almost fully covered by As adatoms is shown in figure 5a. It can be seen that the hydrogen adsorption region can be blocked in different extent and that the surface redox reaction undergone by adsorbed arsenic is spread between 0.3 and 0.7V. This is in contrast with the behavior observed for arsenic adsorbed on a Pt(111) electrode, in which the redox process is essentially limited within a narrow range around 0.5 V. On the other hand two broad contributions are also observed for the redox process of this adatom at Pt(100) [61]. At Pt(110), three peaks are observed at (I) 0.42, (II) 0.56 and (III) 0.66 V in the positive going sweep (figure 5b). If the upper potential limit is maintained at 0,7

V the voltammetric profile remains stable upon cycling. Interestingly, the three peaks grow progressively upon addition of more arsenic on the surface athough peak (I) appears at high surface blockage at the expenses of peak (II). This situation is better observed when desorption of arsenic is forced at high potential: the peak (II) remains more stable in the voltamogram while the state leading to peak (I) readily disappears (figure 5b). In the disappearance of peak (I), peak (II) progressively grows. The peak (III) also diminishes when high potentials are reached but still remains on the voltammogram when the peak (I) has completely disappeared. As the excursion up to 1.0 V is accompanied of adatom desorption, peak (III) can be linked to the oxidation and stripping of arsenic to the solution side. From figure 5b it can be accepted that dissolved arsenic species can redeposit in the negative-going sweep, in addition to the cathodic branches of the redox peaks. It should be remarked that the peak (II) first increases and then decreases, reflecting some interference between peaks (I) and (II) as it happens when As is adsorbed at Pt(111) [61]. In this case it was considered that the peak at lower potentials would correspond to a second structure, growing at the expenses of the previous one, which would correspond to a more diluted and stable adlayer [62]. All these results suggest that peak (II) represents one particular adlayer structure of adsorbed As at Pt(110) at low coverages. Upon addition of more adatoms, a second more unstable and compact structure, peak (II), develops at the surface. Peak (III) is essentially a dissolution peak.

From the voltammetric profiles like those in figures 5a and 5b charge densities can be compared after selective integration of the charge corresponding to the remaining Pt(110) free sites and the oxidation charge involved in the redox processes undergone by the adsorbed arsenic adatoms (figure 6). In the latter case two integration scenarios have been considered: the first one essentially involves the peaks (I) and (II) while the other corresponds to the whole surface oxidation of the adsorbed arsenic, reasonably corrected from substrate

oxidation. The linear plots suggest that the surface stoichiometry is maintained in the whole range of coverage. (Figure 6). The first linear plot follows the experimental relation:

$$Q_{Pt} = Q^{o}_{Pt} - 1.4\ Q_{As} \qquad (6)$$

The slope value could suggest that each As adatom involves 3e in its redox process and blocks two Pt(110) sites of the surface, following a similar interpretation given for the same adatom at Pt(111) taking into account the different substrate symmetry [63]. The second linear plot leads to:

$$Q_{Pt} = Q^{o}_{Pt} - 0.8\ Q_{As} \qquad (7)$$

In this case, the interpretation of the slope value is not straightforward, since contributions from the oxidation of free platinum sites, already observed in the low potential range, could be important as these platinum atoms can be oxidized in the high potential range. In addition, the oxidation of platinum sites, which have been newly liberated form adsorbed arsenic in the same potential excursion, can take place. In any case, the linear plots do not reach the complete blockage of the surface. It seems that some platinum sites remain uncovered so that hydrogen can adsorb at the lowest potential range. In this respect, it should be recalled that hydrogen evolution can take place at As covered Pt(111) [44].

Once characterized, the electrodes were transferred to the formic acid containing cell and their reactivity was checked against its oxidation (Figure 7). In general, the oxidation of the organic molecule is modest, but currents increase with coverage and shifts progressively to lower potentials. It should be highlighted that the upper potential limit was maintained below 0.7 V to avoid As dissolution. For that reason, CO cannot be fully oxidized and the currents in the negative going scan for the Pt(110) electrode are very small. Those small currents are also observed for low amounts of irreversibly adsorbed As. At higher coverage, the increase of the oxidation current is more important and two oxidation peaks are observed at 0.38 and 0.47 V. The potential for the first peak (0.38 V) is more negative than that

corresponding to the surface redox process undergone by the adatom, so that it can be considered that it corresponds to a situation in which formic acid is oxidized at a surface containing few free platinum sites and reduced arsenic adatoms. The second peak, however, could correspond to a surface containing the same few platinum atoms and oxidized arsenic adatoms, likely as $As(OH)_3$ [64]. In this second oxidation peak bifunctional oxidation of adsorbed CO could also be possible.

Poison formation at high arsenic coverage would only be possible if formic acid molecules can reach the platinum substrate atoms, reflecting a strong interaction of formate anions at the surface. However, the current in the foot of the peak (below 0.3 V) was higher in the positive than in the negative-going sweep suggesting negligible poisoning. Despite of that, the voltammograms show typical poisoning hysteresis between both sweeps. It should be remarked that the surface structure could change in some extent, likely because other adsorbates can compete for the surface sites or different adatom mobility in both sweeps.

From the evolution of currents with arsenic coverage (figure 7b), it can be seen a small current increase in figure 7b below $\theta_{As} = 0.5$ with a maximum around $\theta_{As} = 0.25$. This could be related to the growth of the more diluted structure related to peak (II) on the Pt(110) substrate. At higher As coverage, when peak (I) develops and becomes dominant the oxidation current significantly increases. The most striking difference with that observed when atoms are adsorbed at Pt(111) and Pt(100) is that the current densities did not diminish at high adatom coverage. If the oxidation of HCOOH should require the interaction with platinum atoms, it appears that there is place enough at the adatom saturated surface to enable interaction between the solution molecules and the reactive surface sites. This may be a result of the open structure of the substrate and would predict an increasing activity of platinum nanoparticles modified by arsenic, as it was observed in the case of Bi-modified platinum nanoparticles [65] as discussed below. The second oxidation peak at 0.47 V could correspond

to additional contributions coming from CO stripping through oxygen adsorbed on the arsenic adatoms. This bifunctional role of arsenic was proposed earlier by Motoo [66] and it has been pointed out in the stripping of adsorbed CO [67]

In general, the electrochemical behavior of irreversibly adsorbed Sb at Pt(110) is quite similar to that described for As and the adatom surface oxidation also shows several contributions. The main problem is that the adatom redox processes undergone by adsorbed Sb are shifted to higher potentials. The lowest potential peak is centered at 0.55 V, preceded by a small shoulder and is only noticeable at high substrate blockage. It would be similar to the peak (I) in the case of adsorbed As. The main peak, similar to peak (II) in the case of As, appears at 0.7 V and involves a substantially higher charge density (figure 8a). However, as the surface redox process is more shifted to higher potentials, strong interaction with the substrate oxidation potential range takes place. Moreover, severe dissolution of the adatom appears at these high potentials and the voltammetric profiles are not stable upon successive cycles. This would mean that peak (III) contribution is mixed with the previous one. As a result of these complications, the charge balance is not linear and this could mean that the surface processes do not complete in the explored potential range or that the surface stoichiometry changes with coverage (figure 8b).

Despite this lack of surface characterization, adatom coverage can be estimated by surface blocking, following equation (5), and the modified substrates can be checked against formic acid oxidation. It appears that a single oxidation peak is obtained in all cases, the peak currents increase and shift to lower potentials and the maximal reactivity is also obtained with fully covered surfaces (figure 9a). Unlike the case of As in which the peak current densities are modest (slightly more than 1 mA cm^{-2}) the Sb covered Pt(110) electrodes lead to maximal activities around 25 mA cm^{-2}. Also, currents in the positive-going sweep are higher than those recorded in the negative-going one and, unlike the case of Pt(110)-As reported above, there

are no distinct features at low potentials. This would mean that either poison formation cannot take place or that formic acid derived species adsorption can modify the structure of the adlayer during the voltammetric cycle, in such a way that both adlayers could be slightly different from the electrocatalytic point of view and eliminate the presence of the poison at the surface. It should be remarked that two regions are consistently observed in figure 9b: at low Sb coverage there is some noticeable current, but the high activity starts at $\theta_{Sb} > 0.6$. Again, this would would suggest important reactivity at the fully covered surface.

We have obtained similar results with Bi modified Pt(110) electrodes, as it was also reported previously [59]. It appears that Pt(110) covered by adatoms from the nitrogen group exhibit its maximum activity at fully covered surfaces. It should be recalled that such high activity at fully covered electrodes was obtained working with Pt(100)-Bi in the case in which the electrode was cooled in air [14]. After this pretreatment, the electrode contains a high number of surface defects [68] and can serve as a reference model to describe the reactivity of open surfaces like those at Pt(110). In the case of Pt(110)-Bi [59], it was shown that poison formation could take place at the partially covered adatom surfaces at open circuit, its charge diminishing linearly with Bi coverage. This result on poison formation inhibition suggests that the electrocatalytic mechanism could be due to a third body effect. Similar results were obtained with As covered Pt(110) surfaces (not shown), thus pointing to the fact that poison formation inhibition can be successfully achieved at highly covered surfaces. The instability of irreversibly adsorbed Sb precluded this type of experiment in a reliable way, because the poison stripping charge is always accompanied by adatom dissolution.

8. Conclusions

The main conclusion is that the tree basal planes show different reactivity for formic acid oxidation when adatoms of the nitrogen group of the periodic table are irreversibly adsorbed.

For the route through CO, the adatoms always act as a third body. In the case of the Pt(111) electrode, since the defects are responsible of the formation of CO, very small amounts of adatoms are required to completely block CO formation. For the route through the active intermediate, electronic effects seem to play the main role in the increase of intrinsic activity for the Pt(111) electrode [21,15]. The case of Sb at Pt(111) can be considered different because the alloy formation and the subsequent disturbance of the surface structure that seems to be at the origin of the reactivity of nanoparticles [69] [37]. In the case of Pt(100) the adatoms play a third body effect: the poison formation charge decreases linearly with the increase of adatom coverage and the maximum activity is the same, or below, that the intrinsic activity of the unmodified electrode [21]. In both substrates, the reaction seems to take place at the remaining platinum sites uncovered by the adatoms as the formic acid oxidation current drops at the fully covered surfaces in most cases.

At Pt(110) surfaces the most striking difference is that the maximum reactivity for formic acid oxidation is reached at fully covered surfaces. In a rigid adlayer scenario, this could suggest that the covered sites are active, although this would not mean that direct bond of formic acid species with Pt atoms cannot take place. However, at this open surface there is likely room enough for atomic level interaction between the organic molecules and the platinum atoms. In addition, the adatom layer can have some mobility at the open Pt(110) substrate that could result in the appearance of locally less covered sites. At a relatively mobile surface the adatom adlayer structures can be distorted by foreign adsorbates, e.g. formica acid related species, anions or water, in an extent that would be related to the adsorption strength and the size of the modifier. This should be dependent of the applied potential and the perturbation sequence used, justifying the differences observed in both direction sweeps and the inhibition of the spontaneous poison formation at open circuit. Mobility should depend on surface bonding and adatom size. In this respect surface bonding

between As and the Pt(110) substrate could be considered to be the highest, based on electronegativity differences and the adatom size would increase from As to Bi. This could explain the difference in the maximum current densities measured for HCOOH oxidation at Pt(110) electrodes modified by this set of irreversibly adsorbed adatoms.

References

1. Capon A, Parsons R (1973) J Electroanal Chem 45:205-231
2. Willsau J, Heitbaum J (1986) Electrochim Acta 31:943-948
3. Samjeske G, Miki A, Ye S, Osawa M (2006) J Phys Chem B 110:16559-16566
4. Cuesta A, Cabello G, Gutierrez C, Osawa M (2011) Phys Chem Chem Phys 13:20091-20095
5. Chen YX, Heinen M, Jusys Z, Behm RB (2006) Angew Chem Int Edit 45:981-985
6. Chen YX, Ye S, Heinen M, Jusys Z, Osawa M, Behm RJ (2006) J Phys Chem B 110:9534-9544
7. Cuesta A, Cabello G, Osawa M, Gutiérrez C (2012) ACS Catal 2:728-738
8. Osawa M, Komatsu K, Samjeske G, Uchida T, Ikeshoji T, Cuesta A, Gutierrez C (2011) Angew Chem Int Edit 50:1159-1163
9. Chen YX, Heinen M, Jusys Z, Behm RJ (2006) Langmuir 22:10399-10408
10. Chen YX, Heinen M, Jusys Z, Behm RJ (2007) ChemPhysChem 8:380-385
11. Clavilier J, Parsons R, Durand R, Lamy C, Leger JM (1981) J Electroanal Chem 124:321-326
12. Herrero E, Llorca MJ, Feliu JM, Aldaz A (1995) J Electroanal Chem 383:145-154
13. Cuesta A, Escudero Ma, Lanova B, Baltruschat H (2009) Langmuir 25:6500-6507
14. Clavilier J, Fernández-Vega A, Feliu JM, Aldaz A (1989) J Electroanal Chem 261:113-125
15. Clavilier J, Fernández-Vega A, Feliu JM, Aldaz A (1989) J Electroanal Chem 258:89-100
16. Fernández-Vega A, Feliu JM, Aldaz A, Clavilier J (1989) J Electroanal Chem 258:101-113
17. Llorca MJ, Feliu JM, Aldaz A, Clavilier J (1994) J Electroanal Chem 376:151-160
18. Casado-Rivera E, Gal Z, Angelo ACD, Lind C, DiSalvo FJ, Abruna HD (2003) ChemPhysChem 4:193-199
19. Roychowdhury C, Matsumoto F, Mutolo PF, Abruna HD, DiSalvo FJ (2005) Chem Mater 17:5871-5876
20. Alden LR, Han DK, Matsumoto F, Abruña HD, DiSalvo FJ (2006) Chem Mater 18:5591-5596
21. Leiva E, Iwasita T, Herrero E, Feliu JM (1997) Langmuir 13:6287-6293
22. Clavilier J, Armand D, Sun SG, Petit M (1986) J Electroanal Chem 205:267-277
23. Clavilier J, El Achi K, Petit M, Rodes A, Zamakhchari MA (1990) J Electroanal Chem 295:333
24. Herrero E, Fernández-Vega A, Feliu JM, Aldaz A (1993) J Electroanal Chem 350:73-88
25. Herrero E, Feliu JM, Aldaz A (1994) J Electroanal Chem 368:101-108
26. Clavilier J (1987) J Electroanal Chem 236:87-94
27. Grozovski V, Climent V, Herrero E, Feliu JM (2009) ChemPhysChem 10:1922-1926

28. Grozovski V, Climent V, Herrero E, Feliu JM (2010) Phys Chem Chem Phys 12:8822-8831
29. Angelucci CA, Varela H, Herrero E, Feliu JM (2009) J Phys Chem C 113:18835-18841
30. Climent V, Attard GA, Feliu JM (2002) J Electroanal Chem 532:67-74
31. Attard GA, Hazzazi O, Wells PB, Climent V, Herrero E, Feliu JM (2004) J Electroanal Chem 568:329-342
32. Maciá MD, Herrero E, Feliu JM, Aldaz A (1999) Electrochem Commun 1:87-89
33. Maciá MD, Herrero E, Feliu JM, Aldaz A (2001) J Electroanal Chem 500:498-509
34. Maciá MD, Herrero E, Feliu JM (2002) Electrochim Acta 47:3653-3661
35. Grozovski V, Vidal-Iglesias FJ, Herrero E, Feliu JM (2011) ChemPhysChem 12:1641-1644
36. Herrero E, Llorca MJ, Feliu JM, Aldaz A (1995) J Electroanal Chem 394:161-167
37. Climent V, Herrero E, Feliu JM (1998) Electrochim Acta 44:1403-1414
38. Llorca MJ, Herrero E, Feliu JM, Aldaz A (1994) J Electroanal Chem 373:217-225
39. Herrero E, Climent V, Feliu JM (2000) Electrochem Commun 2:636-640
40. Francke R, Climent V, Baltruschat H, Feliu JM (2008) J Electroanal Chem 624:228-240
41. Gisbert R, Climent V, Herrero E, Feliu JM (2012) Journal of Electrochemistry 18:410-426
42. Cuesta A (2006) J Am Chem Soc 128:13332-13333
43. Clavilier J, Feliu JM, Fernandezvega A, Aldaz A (1989) J Electroanal Chem 269:175-189
44. Fernández-Vega A, Feliu JM, Aldaz A, Clavilier J (1991) J Electroanal Chem 305:229-240
45. Feliu JM, Fernandez-Vega A, Orts JM, Aldaz A (1991) JChimPhysPhys-ChimBiol 88:1493-1518
46. Smith SPE, Ben-Dor KF, Abruna HD (1999) Langmuir 15:7325-7332
47. Smith SPE, Abruna HD (1999) J Electroanal Chem 467:43-49
48. Maciá MD, Herrero E, Feliu JM (2003) J Electroanal Chem 554:25-34
49. Souza-Garcia J, Climent V, Feliu JM (2009) Electrochem Commun 11:1515-1518
50. Climent V, Feliu JM (2011) J Solid State Electrochem 15:1297-1315
51. Armand D, Clavilier J (1989) J Electroanal Chem 263:109-126
52. Markovic NM, Grgur BN, Lucas CA, Ross PN (1997) Surf Sci 384:L805-L814
53. Kibler LA, Cuesta A, Kleinert M, Kolb DM (2000) J Electroanal Chem 484:73-82
54. Clavilier J, Orts JM, Gómez R, Feliu JM, Aldaz A (1994) In: Conway BE, Jerkiewicz G (eds), vol 94-21. The Electrochemical Society Proceedings. The Electrochemical Society, INC., Pennington, NJ, pp 167-183
55. Inukai J, Tryk DA, Abe T, Wakisaka M, Uchida H, Watanabe M (2013) J Am Chem Soc 135:1476-1490
56. Wen R, Lahiri A, Alagurajan M, Kuzume A, Kobayashi S-i, Itaya K J Electroanal Chem In Press, Accepted Manuscript
57. Clavilier J, Albalat R, Gómez R, Orts JM, Feliu JM, Aldaz A (1992) J Electroanal Chem 330:489-497
58. Clavilier J, Feliu JM, Aldaz A (1988) J Electroanal Chem 243:419-433
59. Lopez-Cudero A, Vidal-Iglesias FJ, Solla-Gullon J, Herrero E, Aldaz A, Feliu JM (2009) J Electroanal Chem 637:63-71
60. Chang SC, Leung LWH, Weaver MJ (1990) J Phys Chem 94:6013-6021
61. Feliu JM, Fernández-Vega A, Aldaz A, Clavilier J (1988) J Electroanal Chem 256:149-163
62. Dollard L, Evans RW, Attard GA (1993) J Electroanal Chem 345:205-221
63. Zhou WP, Kibler LA, Kolb DM (2004) Electrochim Acta 49:5007-5012
64. Blais S, Jerkiewicz G, Herrero E, Feliu JM (2001) Langmuir 17:3030-3038

65. López-Cudero A, Vidal-Iglesias FJ, Solla-Gullón J, Herrero E, Aldaz A, Feliu JM (2009) Phys Chem Chem Phys 11:416-424
66. Motoo S, Watanabe M (1980) J Electroanal Chem 111:261-268
67. Herrero E, Rodes A, Perez JM, Feliu JM, Aldaz A (1995) J Electroanal Chem 393:87-96
68. Rudnev AV, Wandlowski T (2012) Russ J Electrochem 48:259-270
69. Vidal-Iglesias FJ, López-Cudero A, Solla-Gullón J, Feliu JM (2013) Angew Chem Int Edit 52:964-967

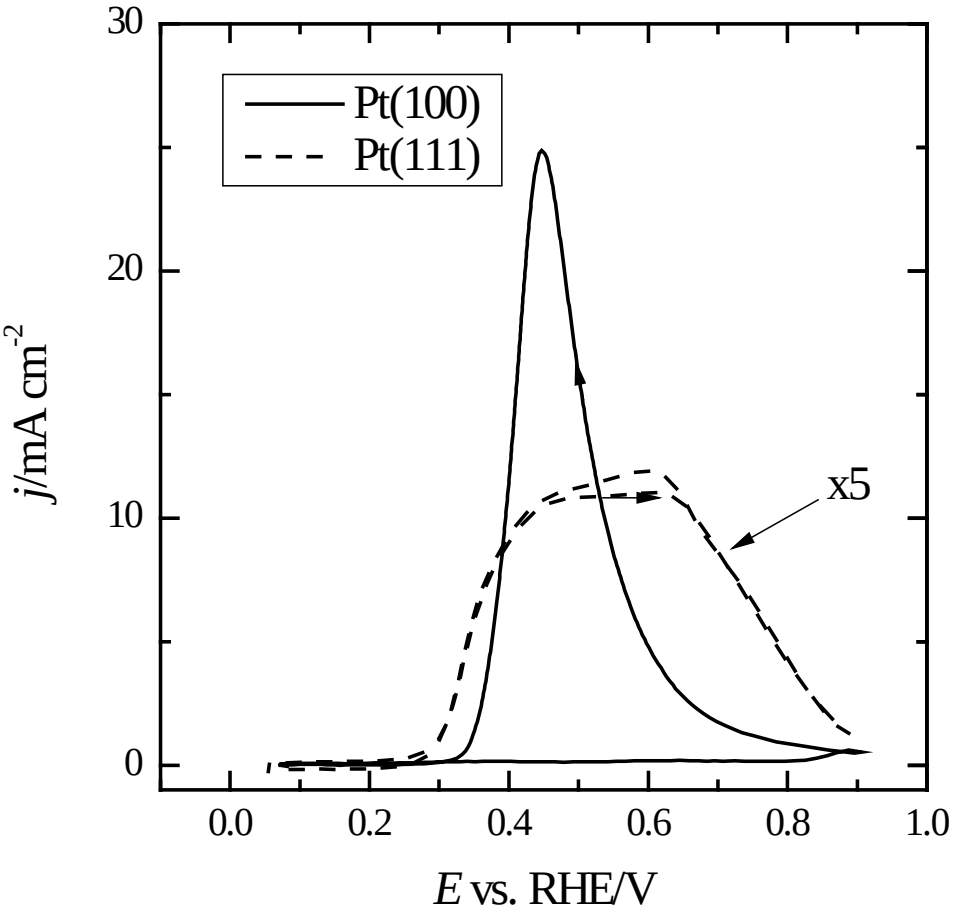

Figure 1. Voltammetric profiles for the Pt(111) and Pt(100) electrodes in 0.5 M H_2SO_4 + 0.1 M HCOOH.

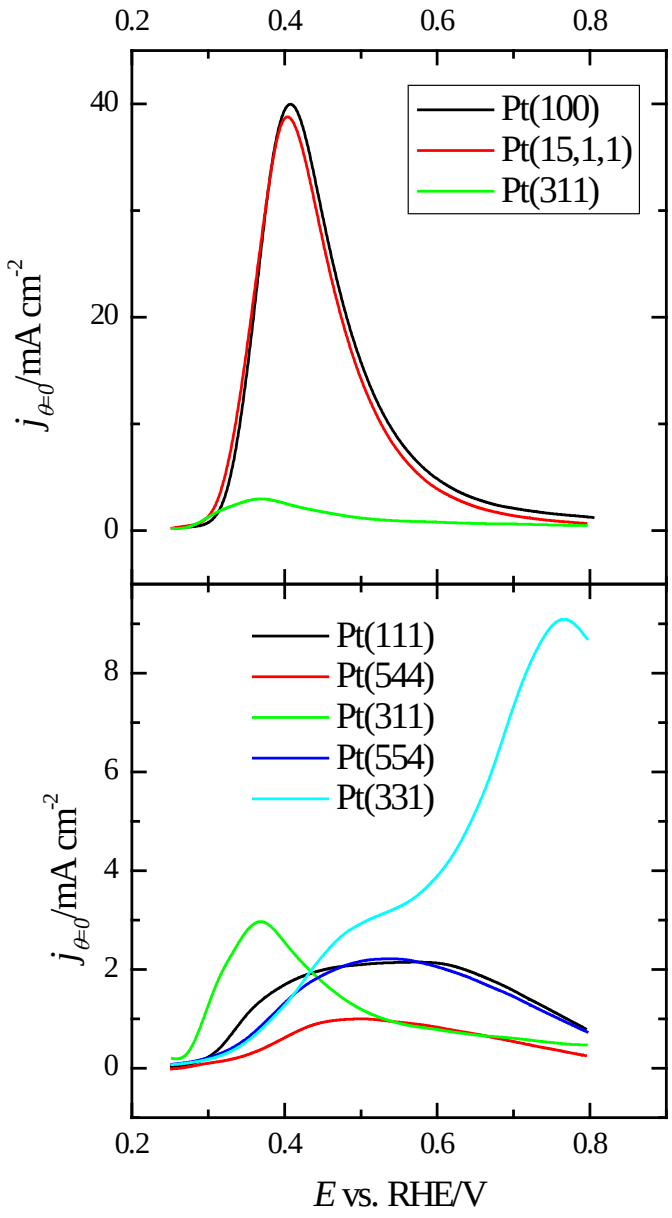

Figure 2. $j_{\theta=0}$ values for different surfaces in 0.5 M H_2SO_4 + 0.1 M HCOOH.

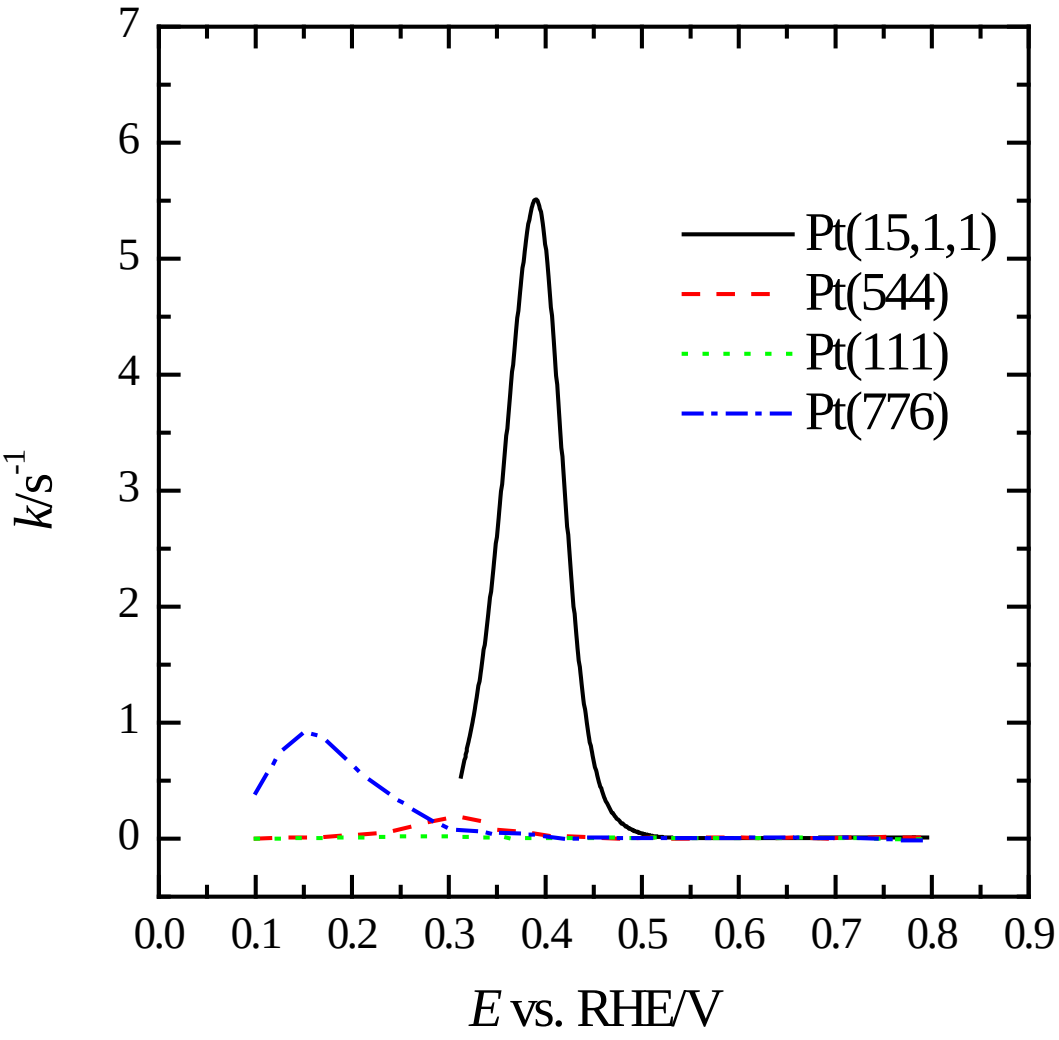

Figure 3. k_{ads} values for different surfaces in 0.5 M H_2SO_4 + 0.1 M HCOOH.

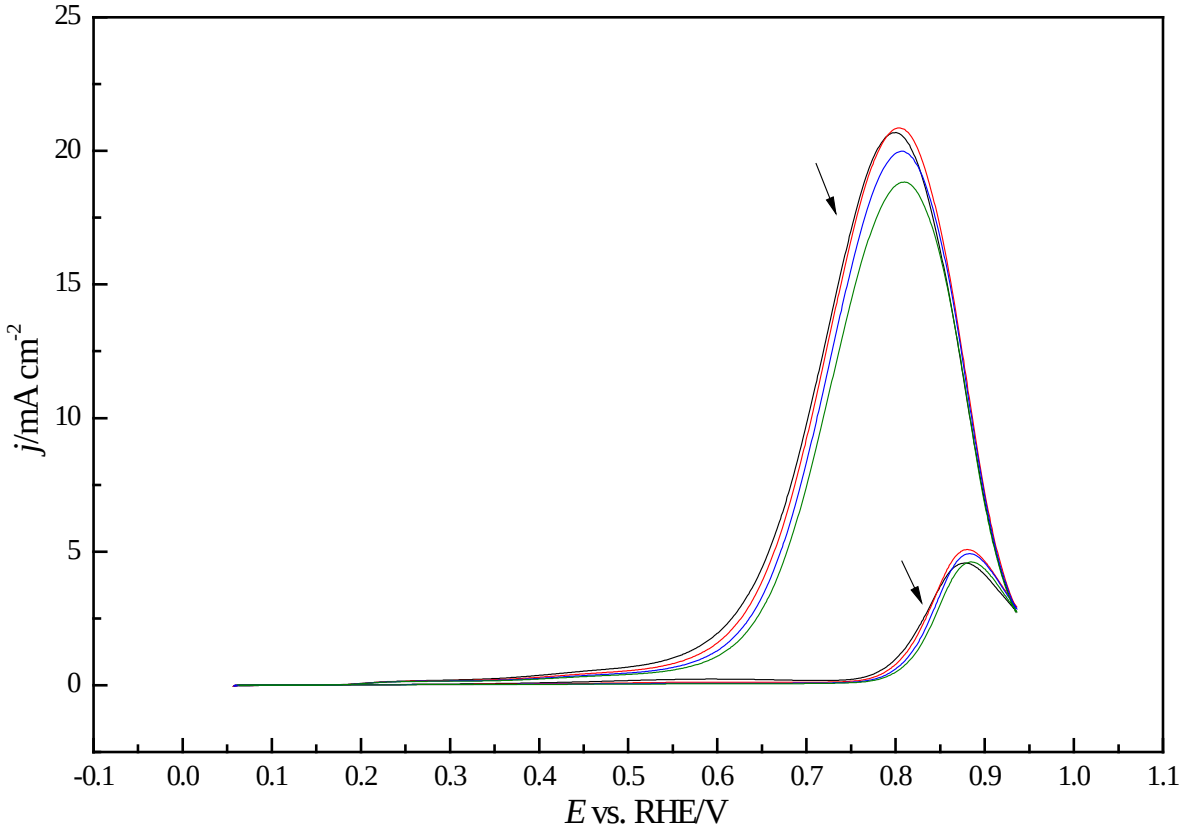

Figure 4. Voltammetric profile of the Pt (110) electrode in 0.5 M H_2SO_4 + 0.1 M HCOOH

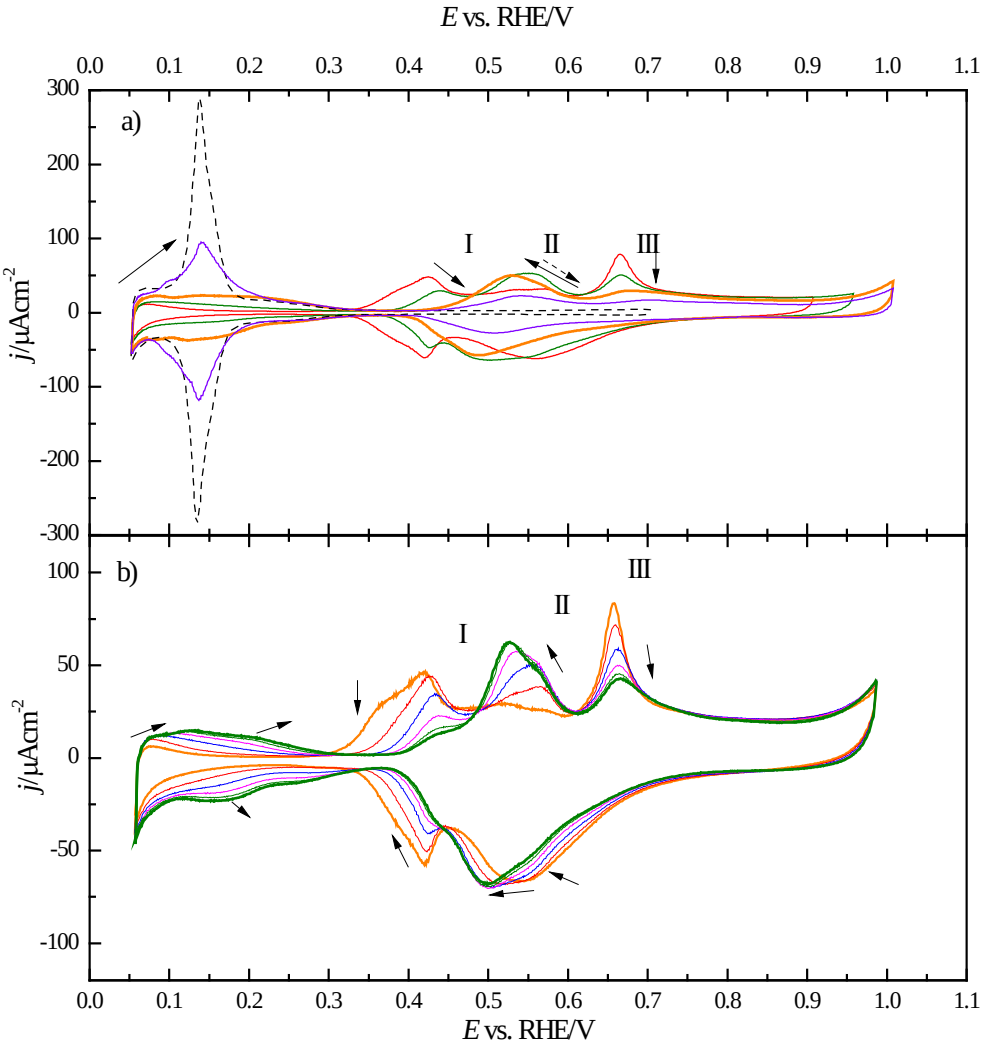

Figure 5. a) Voltammetric profile of the Pt (110)/As electrode for different As coverages in 0.5 M H_2SO_4. The dashed line represents the voltammetric profile of the unmodified Pt(110) electrode. b) Voltammetric profile of desorption of As in Pt (110)/As in 0.5 M H_2SO_4. Scan rate 50mVs^{-1}

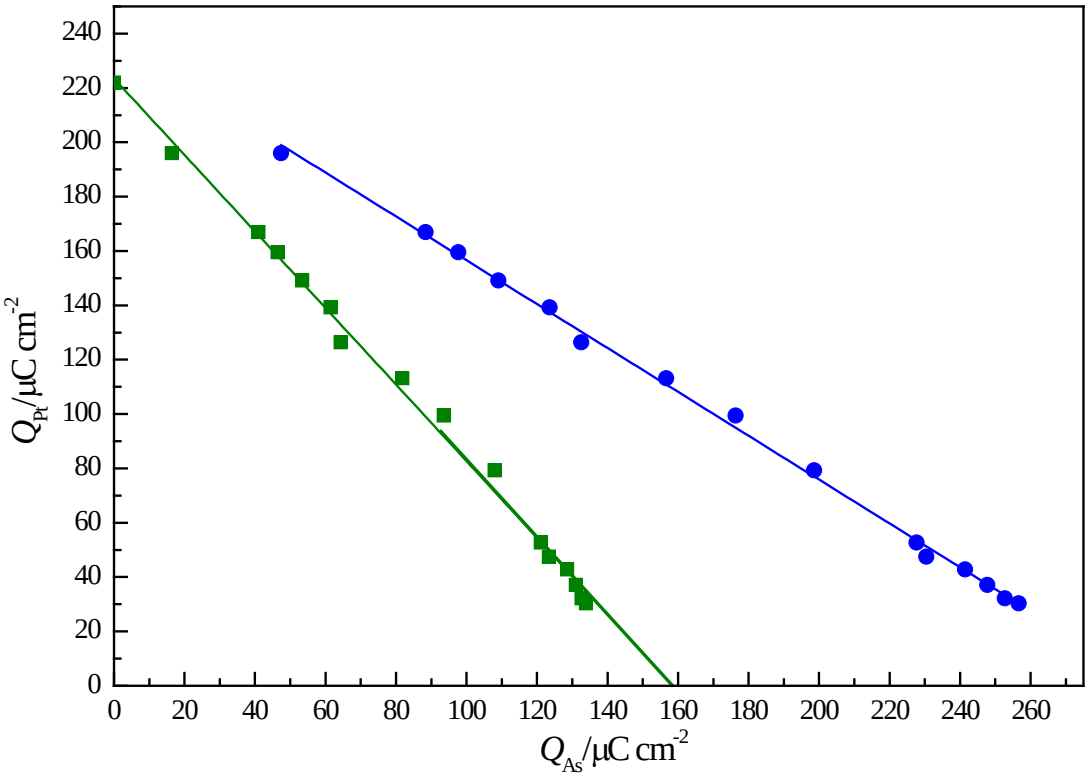

Figure 6. Plots of platinum charge vs. arsenic charge in Pt (110)/As. ● Complete charge of As. ■Arsenic charge associated to the peaks situated at 0.42 and 0.56 V.

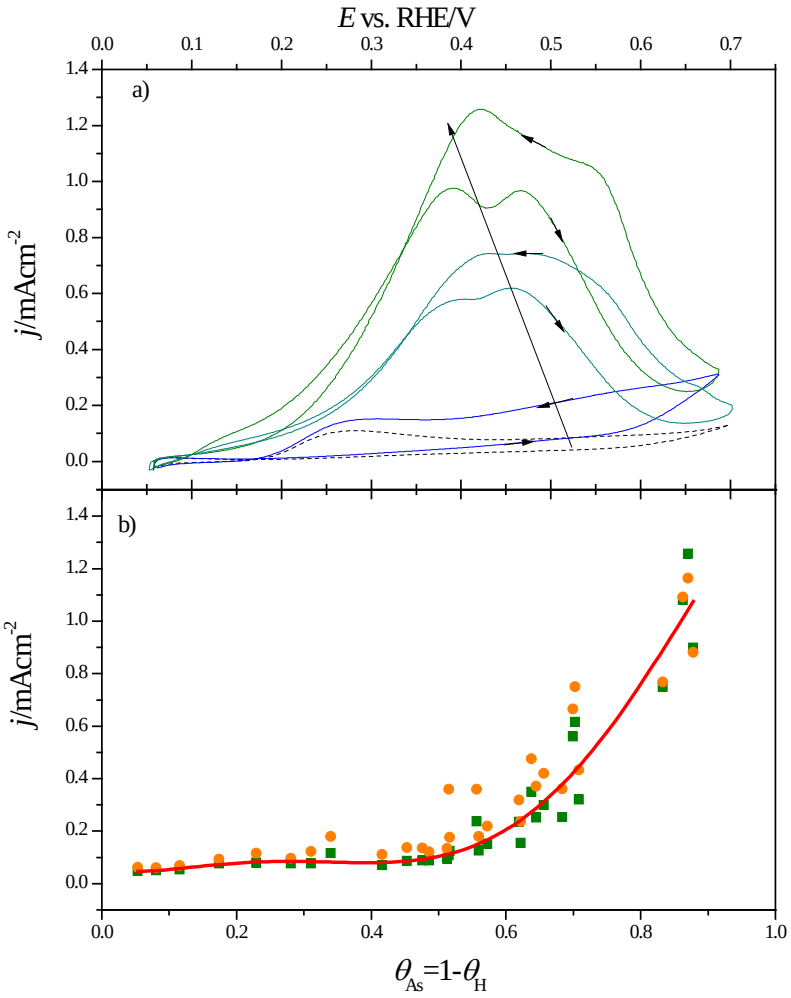

Figure 7. Voltammetric profiles for the Pt(110)/As with different As coverages electrode in 0.5 M H_2SO_4 + 0.25 M HCOOH. Dashed line: voltammetric profiles of the unmodified Pt (110) electrode. Scan rate: 50mVs-1. b) Current densities at (■) 0.42 V and (•) 0.47 V for formic acid oxidation (first scan) vs. arsenic coverage.

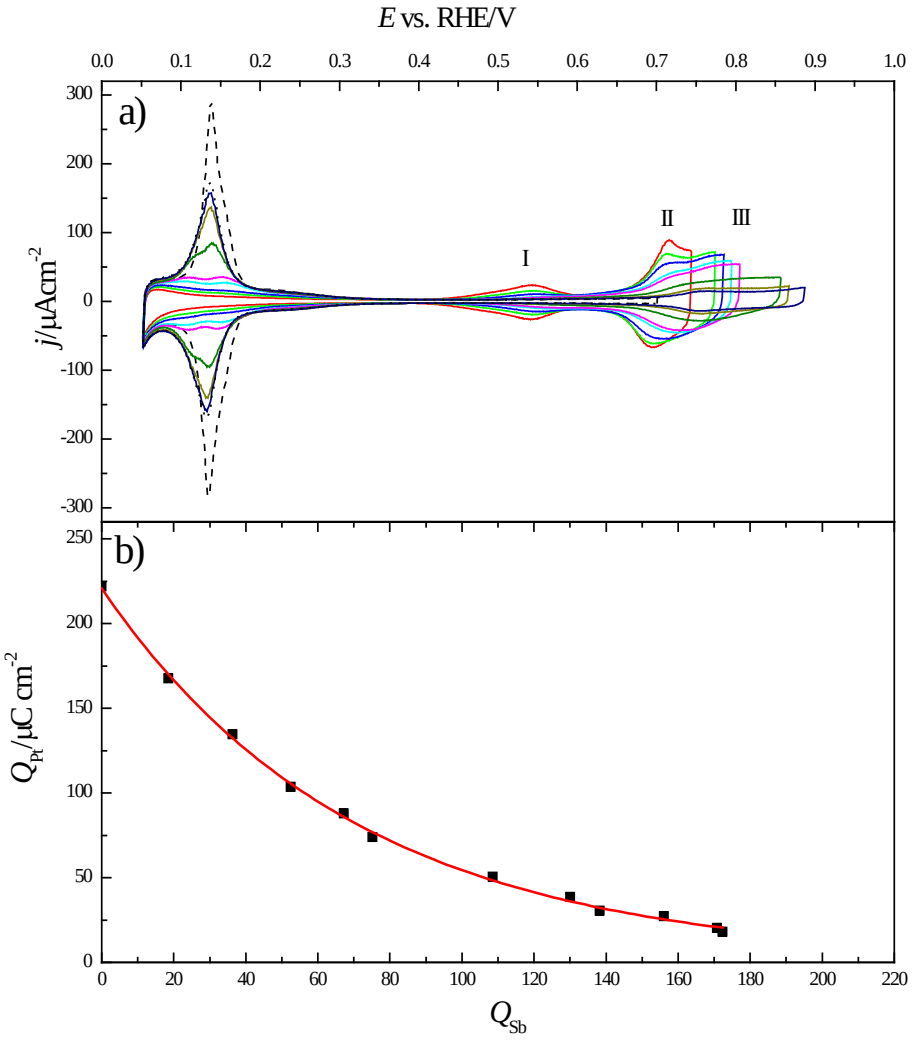

Figure 8. Voltammetric profile of the Pt (110)/Sb electrode in 0.5 M H_2SO_4. The dashed line represents the voltammetric profile of the unmodified Pt(110) electrode. Scan rate 50mVs^{-1}. b) Plot of platinum charge vs. antimony charge in Pt (110)/Sb system

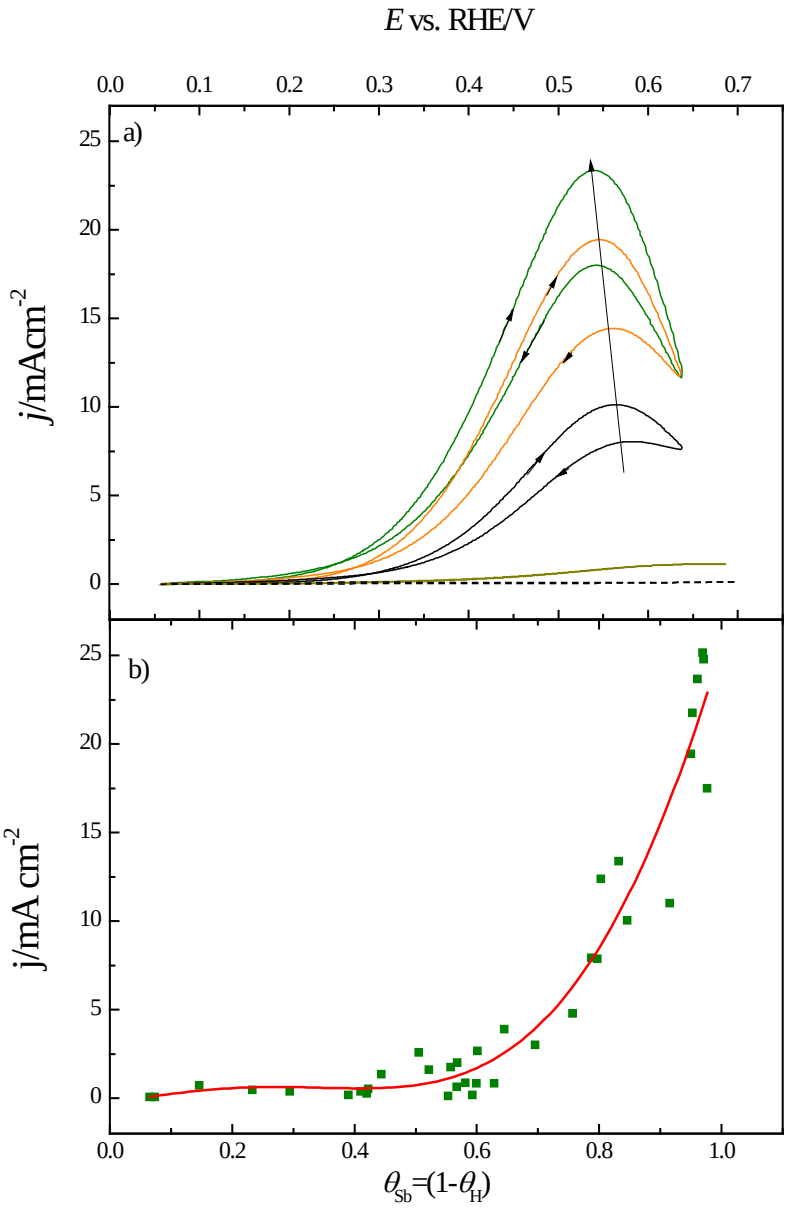

Figure 9. Voltammetric profiles for the Pt(110)/Sb with different Sb coverages electrode in 0.5 M H_2SO_4 + 0.25 M HCOOH. Dashed line: voltammetric profile of the unmodified Pt (110) electrode. Scan rate: 50mVs-1. b) Current densities at 0.55 V for formic acid oxidation (first scan) vs. antimony coverage.